

# Design and Cost Analysis of a Reactive Distillation Column to Produce Ethyl Levulinate Using Excess Levulinic Acid

Igor F. Fioravante, Riann de Q. Nóbrega, Rubens Maciel Filho, and Jean F. Leal Silva

School of Chemical Engineering, University of Campinas (UNICAMP), Campinas, SP, Brazil

\* Corresponding Author: [jeanf@unicamp.br](mailto:jeanf@unicamp.br)

## ABSTRACT

Despite the potential of electrification in transportation, diesel will remain one of the main fuels for decades. The replacement of diesel with biodiesel is one of the solutions to decrease the net emissions of diesel engines. However, biodiesel has limited performance in cold weather and requires fuel additives. In this context, choosing additives from non-edible, inexpensive, renewable sources is important. Ethyl levulinate, an ester derived from levulinic acid that can be produced from sugarcane, is a promising option because it improves the cold-flow properties of fuels and reduces soot emissions. In this work, a reactive distillation column was designed to produce ethyl levulinate. Because of the volatility order of the components involved in this reaction, levulinic acid was chosen as the excess reactant. Production cost was calculated based on ethanol price, capital cost, and operating expenses for several scenarios. The results showed that the optimized reactive distillation column using excess levulinic acid provides a production cost 29% lower than that of a similar esterification process with a continuous stirred tank reactor followed by distillation.

**Keywords:** biofuel, process simulation, biodiesel, ethanol, distillation.

## INTRODUCTION

The biochemical biorefinery platform has been a focus of research because of the potential of using cellulosic sugars in fermentation processes [1]. However, in biomass hydrolysis, part of the sugars is lost in dehydration reactions, yielding furans such as 5-hydroxymethylfurfural and furfural [2]. Generally, furans negatively impact fermentation performance by depleting microorganisms of reducing power [3]. Alternatively, the thermolytic transformation of biomass into products such as furans has great economic potential and avoids fermentation problems [4,5]. Therefore, it is key to explore biorefinery processes based on furans.

Hydrolysis of cellulose yields glucose, which, under severe reaction conditions, is dehydrated to 5-hydroxymethylfurfural (HMF) and subsequently rehydrated to yield levulinic acid and formic acid [6]. Levulinic acid is a  $\gamma$ -keto acid widely recognized as a building block: the carbon chain length and the presence of two organic functions open a myriad of applications [7]. Esters of levulinic acid have a great potential in the fuels market, especially ethyl levulinate [8].

Studies demonstrate that ethyl levulinate enhances combustion efficiency and cold-flow properties of diesel and biodiesel. It also reduces soot emissions in diesel engines [9,10]. The effective replacement of fossil fuels by biofuels depends on the production of high-performance biofuel blends that include key biofuel additives [8], such as ethyl levulinate. Despite the growing interest in electrification, liquid fuels are likely to remain the main energy source for transportation around the world up until 2050 [11], and the decrease in CO<sub>2</sub> emissions by electric vehicles using current battery technology and non-renewable electricity sources is questionable [12]. Additionally, efforts to decarbonize hard-to-electrify sectors, such as the development of marine biofuels, hold a promising future for ethyl levulinate as a fuel additive [13].

The feasibility of ethyl levulinate production on a large scale depends on the production cost of levulinic acid [8]. Production processes for levulinic acid and ethyl levulinate are not well-established in the industry [7]. Besides the bottlenecks in reactor development, there are many subprocesses with cost reduction potential, such as esterification [8]. Process intensification has demonstrated successful results in the esterification of

carboxylic acids in reactive distillation columns [14]. Another important aspect is that distilling ethyl levulinate and levulinic acid requires high temperature, which could otherwise be used to drive the esterification.

The volatility ranking of species is fundamental to deciding upon feed position and size of the reactive section in reactive distillation columns [15,16]. In the case of autocatalysis, all stages are reacting stages. The volatility ranking for the ethyl levulinate reaction represents the least favorable case since both products are the intermediate keys in the distillation [15]. Therefore, conventional approaches for the design of reactive distillation columns cannot be applied thoroughly in this case. A previous study evaluated this system, but it used the traditional excess alcohol strategy, which ended up contributing to increased cost, thus indicating that the opposite approach might be more suitable [17]. Therefore, this work explores an alternative strategy: excess carboxylic acid.

This work investigated the process design of an autocatalyzed reactive distillation column for ethyl levulinate production, assuming an excess carboxylic acid ratio, coupled with techno-economic analysis. A surrogate model was used to optimize operating conditions to improve economic indicators. The developed process design was then compared to a conventional autocatalyzed esterification process working at similar conditions.

## METHODOLOGY

Process design consisted of three steps: i) initial assessment based on thermodynamics and kinetic limitations; ii) use of design of experiments to obtain a surrogate model for optimization; and iii) simulation and assessment of optimized operating conditions.

Thermodynamic and kinetic analyses were conducted using Aspen Plus 14 (AspenTech, Inc., USA, 2022). Carboxylic acids associate in the vapor phase and lead to a negative deviation in the molar volume, which is accounted for by the Hayden-O'Connell equation of state [18]. The NRTL (non-random, two-liquid) model was chosen for the liquid phase; binary interaction parameters of the water-ethanol pair were obtained from the Aspen Plus 14.0 database, and parameters for the other pairs were obtained from Resk *et al.*, 2014 [18].

The conversion of levulinic acid at equilibrium conditions was calculated using the *REquil* model in Aspen Plus, which considers chemical equilibrium conditions. A similar analysis was carried out considering reaction kinetics using an *RCSTR* model (residence time: 60 min). The esterification reaction is presented in Figure 1, and the kinetics of the autocatalyzed reaction is described by Eq. (1). In this equation, the driving force is the concentration of species on molar basis ( $C_{LA}$  for levulinic acid,  $C_{EtOH}$  for ethanol,  $C_{EL}$  for ethyl levulinate,  $C_w$  for water), mediated by the equilibrium constant  $K_{eq}$ . Other factors

include the pre-exponential factor ( $k_0$ , 100 m<sup>3</sup>/kmol.s), the activation energy ( $E_A$ , 49 kJ/mol), the universal gas constant ( $R$ ), and the temperature ( $T$ ) [19].

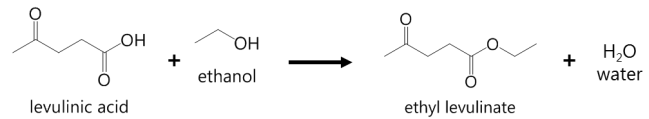


**Figure 1.** Esterification of levulinic acid with ethanol.

$$r = k_0 \exp\left(\frac{-E_A}{RT}\right) \left(C_{LA}C_{EtOH} - \frac{C_{EL}C_w}{K_{eq}}\right) \quad (1)$$

Optimization was carried out using a surrogate model based on a central composite design with face-centered star points to facilitate convergence. This approach also allows the statistical analysis of the process. The following parameters of the reactive distillation column were considered in the surrogate model: weir height ( $WH$ ), ethanol to levulinic acid ratio ( $ELA$ ), number of stages ( $NST$ ), and reboiler temperature ( $RT$ ). The column diameter was calculated in Aspen Plus (Fair correlation). The column diameter and weir height determine the liquid holdup needed for the reaction. The design space (Table 1) was defined based on simulations of distillation columns (shortcut method) for feeds in the conversion range of 10–100% of the reaction depicted in Figure 1.

**Table 1:** Design space used in the process optimization.

Variable	-1	0	+1
WH (mm)	100	150	200
ELA	0.2	0.6	1.0
NST	20	40	60
RT (°C)	160	180	200

The design included 25 cases since there are four factors and the process was simulated (replicates to calculate error are unnecessary). For each case, the cost of ethyl levulinate ( $CEL$ ) was calculated.  $CEL$  is defined as the sum of operating and capital expenses divided by the production rate of ethyl levulinate (excluding the cost of levulinic acid),  $x$  represents each coded variable, and  $c$  represents the coefficients of the surrogate model. Capital cost was calculated according to the literature [20] and added to the  $CEL$  after a discount rate of 10% on an equipment life span of 10 years. The material of construction was SS316. The column uses bubble cap trays. The statistical analysis was completed using the software Statistica 13.3 (TIBCO Software Inc., Palo Alto, USA, 2017). Utility cost was estimated according to the literature [21]. Ethanol cost was based on the monthly average from 2019 to 2023 [22]. Data of the 25 cases were regressed into the surrogate model shown in Eq. (2).

$$CEL = c_0 + \sum_{i=1}^n c_i x_i + \sum_{i=1}^n c_{ii} x_i^2 + \sum_{i=1}^n \sum_{j \geq i}^n c_{ij} x_i x_j \quad (2)$$

Levulinic acid (recycled and fresh) was fed at 90 °C to the top tray of the reactive distillation column (*RadFrac* block). The levulinic acid to ethanol ratio was adjusted via the Design Spec tool of Aspen Plus according to each simulated case. Ethanol (1.5 bar, 150 °C) was fed at the bottom of the reactive distillation column as vapor. The esterification reaction was set to occur on all stages with kinetics described by Eq. (2). Residence time in each tray was set according to the calculated velocity obtained as a function of the diameter of the column. As a simplification due to the volume of simulations, vapor-liquid equilibrium was reached in any stage of the column.

The bottoms flow rate was fixed via the Calculator tool of Aspen Plus equal to 99.5% of the levulinic acid and ethyl levulinate entering the column. The reflux ratio was varied to recover a bottom product containing 99.9% levulinic acid and ethyl levulinate. The distillate contained water and unreacted ethanol. Ethanol and water were separated using molecular sieves. For this processes, operating conditions and investment were based on data available in the literature [23]. Unreacted ethanol was recycled into the column. The bottom stream of the reactive distillation column was distilled to separate ethyl levulinate and levulinic acid, the latter recycled to the esterification process. This last column was designed using shortcut methods. Ethyl levulinate was obtained at a purity of 99.5 wt%.

Other parameters considered in the process simulation include: pressure in the condenser of the reactive distillation column was varied to attain any specified *RT* (design variable); stage pressure drop was 4–6 mbar (depending on *RT*); tray spacing of 0.6 m in both the reactive distillation column and second distillation column; residence time in the reflux drum and reboiler sump was 5 min; streams of wastewater, levulinic acid, and ethyl levulinate leaving the second column and the ethanol dehydration were used in heat integration to preheat ethanol, considering a temperature approach of 10 °C in a series of *HeatX* models; streams of ethyl levulinate and wastewater were cooled to 50 °C; service life of molecular sieves used in dehydration of ethanol was equal to the project lifespan (10 years); saturated steam was available at 28 bar and 8 bar (returning as saturated liquid); cooling water was available at 30 °C (returning at 40 °C); chiller water was available at 0 °C (returning at 10 °C). The system was sized to a production rate of 100 kt/y of ethyl levulinate, operating 8000 h per year.

The validity of the surrogate models was attested using the Fisher test with the analysis of variance table. The surrogate model was used as the objective function to minimize *CEL* using the gradient-based method of the Solver tool of Microsoft Excel. The obtained results were then simulated to validate the optimization, and the reactive distillation column was analyzed in terms of profiles (composition, temperature, etc.).

For the sake of comparison, an esterification via a conventional process composed of a stirred tank reactor followed by a distillation train was simulated as well. The reaction kinetics were the same as Eq. (2). Among the variables of Table 1, only *ELA* was considered an optimization variable in this scenario. The optimum was searched in the range of 0.6 to 1.4. The reactor temperature was fixed at 200 °C to ensure a high reaction rate, and pressure was chosen to ensure the reactor operated at subcooled conditions. The residence time was varied to attain 99% of the equilibrium conversion at any specified *ELA* condition.

## RESULTS AND DISCUSSION

### Basis for process design

According to Figure 2a, increasing the *ELA* from 1 to 2 increases the conversion at equilibrium conditions on average by 13% (temperature range of 0–200 °C). Regarding the kinetics of the autocatalyzed reaction (Figure 2b), increasing the *ELA* from 1 to 2 increases the conversion in a reaction time of 20 minutes at 200 °C by 31% and at 150 °C by 38%. Different from *ELA*, temperature has little effect over the maximum possible conversion at equilibrium conditions (Figure 2a). However, high temperature is fundamental to achieving desirable conversion in the autocatalyzed reaction (Figure 2b). This scenario – high *ELA* and high temperature – corresponds to the conditions expected at the bottom of the distillation column since the unreacted levulinic acid is in contact with the total feed of ethanol at the reboiler temperature.

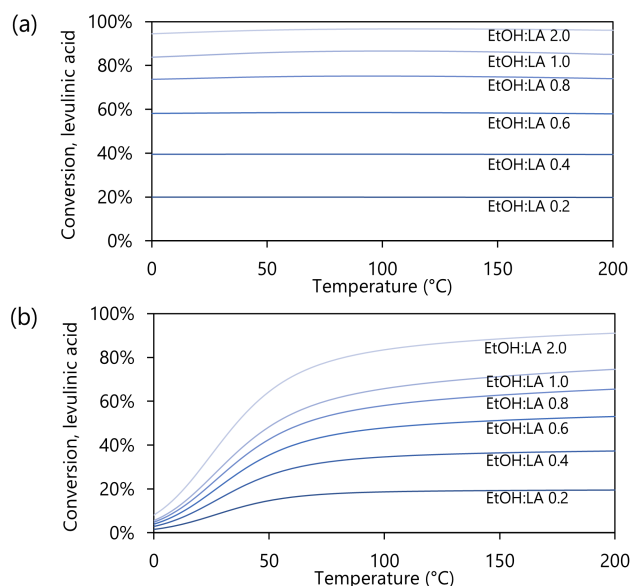


**Figure 2.** Conversion of levulinic acid at equilibrium and at 60 minutes for different temperatures and ethanol to levulinic acid (EtOH:LA, *ELA*) ratios of 0.2 to 2.0.

The absence of an efficient catalyst and the unfavorable volatility ranking (products are intermediate keys) gives rise to a problem: a design to attain complete conversion of reactants is unfeasible. Moreover, other two factors play an important role: i) ethanol and water present an azeotrope, which requires special treatment, and ii) the light key components are considerably more volatile than the heavy key components. Therefore, the design used in this work was based on the potential of contacting a high excess of reactants on both the top and bottom of the column to drive conversion.

### Surrogate model

Simulations were run considering the design of experiments, and the resulting *CEL* was calculated for each case. Ethanol accounts for 83% of the *CEL*. The data were analyzed with a confidence interval of 95%. The  $R^2$  (coefficient of determination) was 0.976. The calculated F-test ratio in both scenarios exceed 10 by a large margin, thus indicating that the surrogate model is useful for prediction and, consequently, can be used in process optimization despite being a simplistic approach. Figure 3 shows the response surfaces obtained from the data.

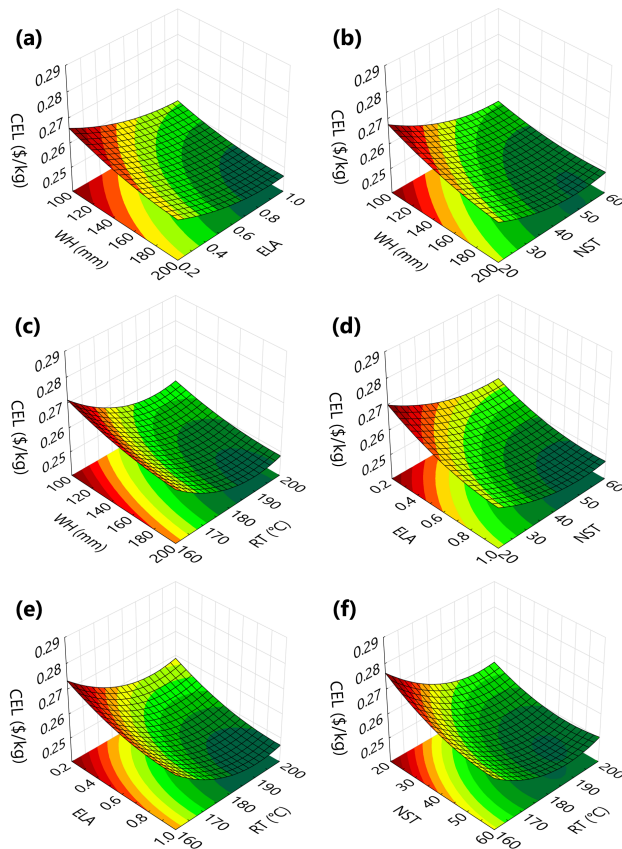


**Figure 3.** Response surfaces: a) *WH* vs. *ELA*, b) *WH* vs. *NST*, c) *WH* vs. *RT*, d) *ELA* vs. *NST*, e) *ELA* vs. *RT*, and f) *NST* vs. *RT*. In each case, values of the other variables were fixed at their central points.

Based on the surrogate model, conditions that minimize *CEL* are as follows: *WH* of 185 mm, *ELA* of 0.93, *NST* of 46, and *RT* of 190 °C. The *CEL* was estimated via process simulation based on these conditions: \$0.243 kg<sup>-1</sup>. The value predicted by the model differs only by 0.26% from the value calculated via process simulation. This demonstrates the potential of the surrogate model in predicting the results of the rigorous model.

Analysis of graphs a, b, and c of Figure 3 shows that *CEL* decreases when *WH* is increased (n.b.: the axis direction in some graphs was inverted to aid visualization). High *WH* means that the column needs to be reinforced to withstand the large liquid holdup, which in turn means an increase in capital cost. However, the obtained increase in residence time as a consequence of the high *WH* demonstrated to be effective in reducing the *CEL*. The increase in *NST* also contributes to lower *CEL*, as observed in graphs b, d, and f of Figure 3. However, it can be observed that this effect levels off around 50 stages, with a clear minimum. Similar behavior occurs for *RT* (graphs c, e, and f of Figure 3) around 190-200 °C. Even though high temperature substantially increases the conversion rate, it demands more corrosion allowance, which increases capital cost.

Graphs a, d, and e of Figure 3 demonstrate the effect of *ELA*. Excess of one reactant is interesting to achieve higher conversion at equilibrium conditions (Figure 1). However, since the reaction is autocatalyzed, the system never reaches near-equilibrium conditions. Therefore, the equilibrium is not a limitation to justify the use of high excess of any reactant. It was observed that the extreme condition of large excess of one reactant implies in a low concentration of the other, which in turn decreases the reaction rate.

### The optimized design

The design of the optimized esterification process is presented in Figure 4. The reaction rate (Figure 5a) averaged 1.9 kmol h<sup>-1</sup> on column trays. The condenser drum, which operated at low temperature and a residence time of 5 min, presented a reaction rate of 0.001 kmol h<sup>-1</sup> mainly because of the low levulinic acid concentration (Figure 5b). The reboiler has by far the highest temperature and it presented a reaction rate in the same order as the rest of the column (2.0 kmol h<sup>-1</sup>) despite the low ethanol concentration. Ethanol was fed one stage above and preferentially flows to the upward stages.

Temperature (Figure 5a) grew steadily from top to bottom in almost the entirety of the column, growing rapidly after ethanol concentration in the liquid phase peaks (stages 41-45). The slow increase in temperature is a consequence of volatility and concentration of components along the column. In bottom stages, the concentration of components is ranked as ethyl levulinate, levulinic acid, and ethanol, with the latter (the lightest component)

reaching concentrations up to 9 mol% in the liquid phase (Figure 5b). In the top stages, ethyl levulinate has a low concentration, at the same region where water concentration peaks. Therefore, the change in temperature is both a consequence of column fractionation and reaction, which is an expected behavior. Similar behavior was observed by the other investigators [16].

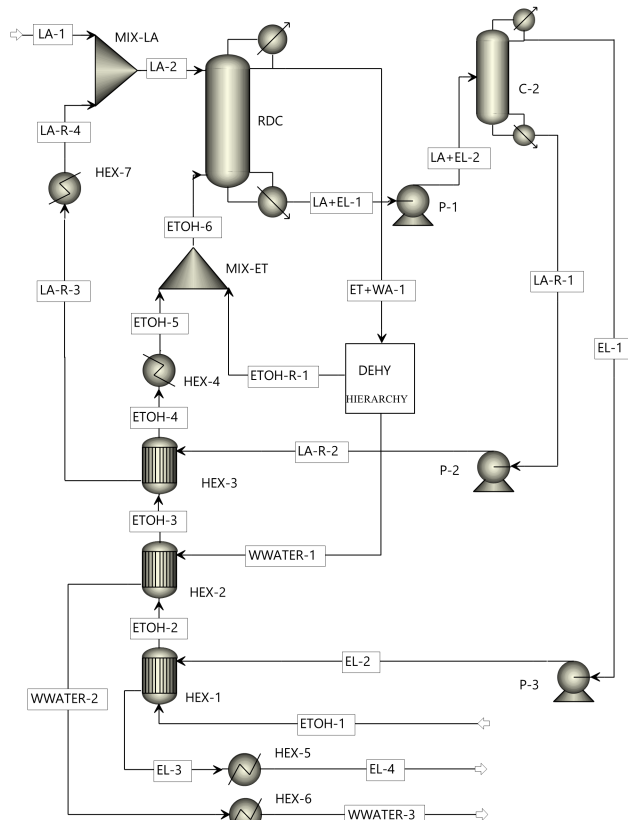


**Figure 4.** Simulation flowsheet of the optimized process.

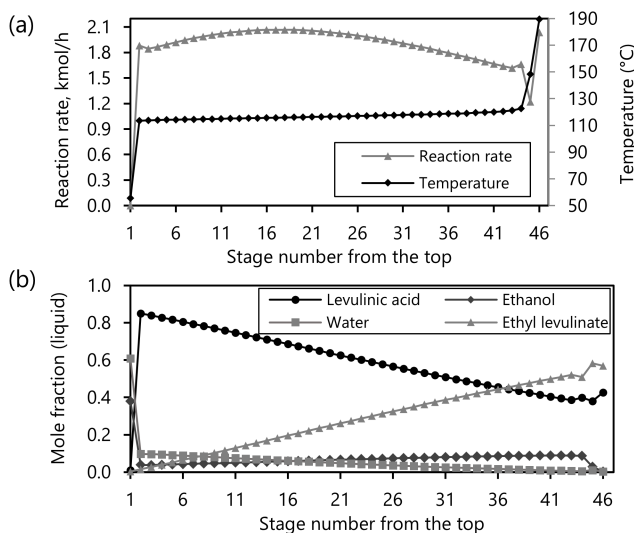


**Figure 5.** Simulation flowsheet of the optimized process.

The reaction rate is almost constant throughout the column, decreasing towards the bottom (stages 18-46). Consequently, concentration profiles (Figure 5b) are nearly straight lines. The concentration profile of levulinic acid in the liquid phase decreases according to the reaction rate because levulinic acid flows downward, its concentration in the vapor phase is too low. As the reaction slows down in the bottom stages, the concentration of levulinic acid tends to become constant.

Stages 45 and 46 have temperatures beyond 130 °C. High temperature is expected at the bottom stages because of the reboiler, thus contributing to a higher reaction rate as the ester product becomes more concentrated. On the other hand, trays on stages 2-40 operate between 110-120 °C. This result suggests that the trays of the upper stages of the column require less corrosion allowance, which could reduce their cost.

### Comparison to other process option

Optimization via a surrogate model of the conventional setup (stirred tank reactor followed by distillation) indicated that an *ELA* of 1.09 results in a *CEL* of \$0.253 kg<sup>-1</sup>, 4.05% higher than that of the optimized reactive distillation. Ignoring ethanol cost in both scenarios, the difference regarding equipment cost and operating expenses becomes more evident: the conventional process costs 41% more than the reactive distillation process.

## CONCLUSIONS

This work assessed a reactive distillation column that produces ethyl levulinate via autocatalyzed esterification of levulinic acid. Optimized operating conditions were estimated via a surrogate model obtained via design of experiments. Statistical analysis demonstrated that the quadratic surrogate model has desirable confidence level inside the explored data space. Optimized parameters indicated that the lowest cost of ethyl levulinate was obtained at high reboiler temperature, high number of stages, high liquid holdup, and ethanol to levulinic acid molar ratio slightly lower than one. Single-pass conversion was not feasible because of the low reaction rate and recycle of unconverted reactants showed a large impact on operating costs. Nevertheless, the design was effective: the cost of ethyl levulinate on a conventional set of stirred tank reactor and distillation train excluding ethanol and levulinic acid costs was estimated to be 41.1% higher than the upgrading cost using a reactive distillation column. These results indicate the opportunity of carrying out the esterification of levulinic acid in a reactive distillation column.

## ACKNOWLEDGEMENTS

The authors acknowledge the São Paulo Research

## REFERENCES

1. Leal Silva JF, Nakasu PYS, Costa AC da, Maciel Filho R, Rabelo SC. Techno-economic Analysis of the Production of 2G Ethanol and Technical Lignin via a Protic Ionic Liquid Pretreatment of Sugarcane Bagasse. *Ind Crops Prod* 189:115788 (2022)
2. Clauser NM, Gutiérrez S, Area MC, Felissia FE, Vallejos ME. Small-sized biorefineries as strategy to add value to sugarcane bagasse. *Chem Eng Res Des* 107:137–46 (2016)
3. Sun C, Liao Q, Xia A, Fu Q, Huang Y, Zhu X, et al. Degradation and transformation of furfural derivatives from hydrothermal pre-treated algae and lignocellulosic biomass during hydrogen fermentation. *Renew Sustain Energy Rev* 131:109983 (2020)
4. Leal Silva JF, Mariano AP, Maciel Filho R. Less severe reaction conditions to produce levulinic acid with reduced humins formation at the expense of lower biomass conversion: Is it economically feasible? *Fuel Commun* 9:100029 (2020)
5. Yong KJ, Wu TY, Lee CBTL, Lee ZJ, Liu Q, Jahim JM, et al. Furfural production from biomass residues: Current technologies, challenges and future prospects. *Biomass and Bioenergy* 161:106458 (2022)
6. Lopes ES, Silva JFL, do Nascimento LA, Bohórquez JFC, Lopes MS, Tovar LP, et al. Feasibility of the conversion of sugarcane molasses to levulinic acid: Reaction optimization and techno-economic analysis. *Ind Eng Chem Res* 60:15646–57 (2021)
7. Di Menno Di Bucchianico D, Wang Y, Buvat JC, Pan Y, Casson Moreno V, Leveneur S. Production of levulinic acid and alkyl levulinates: a process insight. *Green Chem* 24:614–46 (2022)
8. Leal Silva JF, Grekin R, Mariano AP, Maciel Filho R. Making Levulinic Acid and Ethyl Levulinate Economically Viable: A Worldwide Technoeconomic and Environmental Assessment of Possible Routes. *Energy Technol* 6:613–39 (2018)
9. Chernyshev VM, Kravchenko OA, Ananikov - VP, Ramanathan NR, K Balasekhar CS, Frigo S, et al. Utilisation of Ethyl Levulinate as Diesel Fuel Additive. *J Phys Conf Ser* 2648:012072 (2023)
10. Wu P, Miao C, Zhuang X, Li W, Tan X, Yang T. Physicochemical characterization of levulinate esters with different alkyl chain lengths blended with fuel. *Energy Sci Eng* 11:164–77 (2023)
11. Dale S, Smith TD. Back to the future: electric vehicles and oil demand BP Group chief economist BP Global Oil Market Economist. London (2016)
12. Qiao Q, Zhao F, Liu Z, Jiang S, Hao H. Cradle-to-gate greenhouse gas emissions of battery electric and internal combustion engine vehicles in China. *Appl Energy* 204:1399–411 (2017)
13. Oppong F, Xu C, Li X, Luo Z. Esters as a potential renewable fuel: A review of the combustion characteristics. *Fuel Process Technol* 229:107185 (2022)
14. Lee H-Y, Hsiao T-L, Ng DKS, Elyas R, Chen C-L, Elms RD, et al. Design and Simulation of Reactive Distillation Processes. Elsevier, p. 311–53, (2017)
15. Tung S-T, Yu C-C. Effects of relative volatility ranking to the design of reactive distillation. *AIChE J* 53:1278–97 (2007)
16. Novita FJ, Lee H-Y, Lee M. Energy-Efficient Design of an Ethyl Levulinate Reactive Distillation Process via a Thermally Coupled Distillation with External Heat Integration Arrangement. *Ind Eng Chem Res* 56:7037–48 (2017)
17. Leal Silva JF, Wolf Maciel MR, Maciel Filho R. Optimization of High Temperature Reactive Distillation for Production of Ethyl Levulinate. *Chem Eng Trans* 69:379–84 (2018)
18. Resk AJ, Peereboom L, Kolah AK, Miller DJ, Lira CT. Phase Equilibria in Systems with Levulinic Acid and Ethyl Levulinate. *J Chem Eng Data* 59:1062–8 (2014)
19. Bankole KS, Aurand GA. Kinetic and Thermodynamic Parameters for Uncatalyzed Esterification of Carboxylic Acid. *Res J Appl Sci Eng Technol* 7:4671–84 (2014)
20. Turton R, Shaeiwitz JA, Bhattacharyya D, Whiting WB. Analysis, Synthesis, and Design of Chemical Processes. Pearson Education (2018)
21. Ulrich GD, Vasudevan PT. How to Estimate Utility Costs. *Chem Eng* April:66–9 (2006)
22. Brazilian Ministry of Economy. Comex Stat. <http://comexstat.mdic.gov.br/en/home> (accessed May 16, 2024).
23. Kang Q, Huybrechts J, Van der Bruggen B, Baeyens J, Tan T, Dewil R. Hydrophilic membranes to replace molecular sieves in dewatering the bio-ethanol/water azeotropic mixture. *Sep Purif Technol* 136:144–9 (2014)

© 2025 by the authors. Licensed to PSEcommunity.org and PSE Press. This is an open access article under the creative commons CC-BY-SA licensing terms. Credit must be given to creator and adaptations must be shared under the same terms. See <https://creativecommons.org/licenses/by-sa/4.0/>

